DYNAMIC ANALYSIS OF A FLARE TOWER IN OFF-SHORE PLATFORMS

Tomaz de Paula Drumond
Universidade Federal de Minas Gerais/UFMG, Escola de Engenharia, Belo Horizonte, MG, Brazil
E-mail: tomdrud@ufmg.br

Daniel Nelson Maciel
Universidade Federal do Rio Grande do Norte/UFRN, Lagoa Nova, Natal, RN, Brazil
E-mail: dnmaciel@ect.ufrn.br

Marcelo Greco
Universidade Federal de Minas Gerais/UFMG, Escola de Engenharia, Belo Horizonte, MG, Brazil
Corresponding author: E-mail: mgreco@dees.ufmg.br

Abstract: Since deepwater petroleum deposits were discovered in 2008, many projects of off-shore platforms were made in Brazil. Therefore, it is necessary to know better the behavior of structural elements that are used on these platforms, both under static and under dynamic conditions. The present work deals with the dynamic analysis of a flare tower, which is a truss structure attached to these platforms, where gases with no industrial application are burned. As a result of the burn, shock waves generated during the process reach the flare tower structure, causing the occurrence of blast loads. On the present work, the behavior of the flare tower under blast loadings was analyzed. The structure was considered as a space truss due to its geometry and its joints. New flare tower dimensions were calculated and equivalent blast loading values were estimated. These values were established as initial conditions; stress and strainvalues in the finite elements are calculated. Thus, it was possible to evaluate if the structure of the flare tower would fail and the critical conditions on the structure could be identified. Results indicate that the structure is in safe conditions up to a limited period of time, due to the fatigue of materials.

Keywords: Explosion effects; Nonlinear analysis; Space truss.

Received: April, 27 2016 - Accepted: January, 13 2017

INTRODUCTION

Since more deepwater petroleum deposits were discovered in Brazilian coast, the process of petroleum extraction was intensified, mainly by the build of new platforms. Thus, it is necessary to make an analysis to know better the elements on the maritime units that make the petroleum extraction. Among the structures in the extraction platforms, there is the flare tower, a truss structure that supports the flare where useless gases, arising from the processing of oil, are burned. This structure is extremely high to avoid the exposure of people and others equipment to the flame located at the top of the burner and the heat generated in the production plant. During the burning process at the flare tower shock waves are generated and they affect the truss structure that supports the burner. According to Kinney and Graham (1985), the generated shock waves are essentially immaterial andare generated by sudden releases of energy that occur during the burning process.

The support structure can be characterized as space truss due to its geometry and its joints. There are very few references available among the literature specifically dedicated to the flare tower analysis. The main available references for this kind of analysis are mainly technical standards, such as American Petroleum Institute (2007); TNO PrinzMauritz Institute (1997); Gilmer et al. (2003). One of the few papers available among the literature regarding this issue, Singhal (1989), is dedicated to analyze the radiations and the noise caused by flaring of the produced gas. According to Singhal (1989), the stack-enclosed flare system is studied, considering steady-state analysis and null wind velocity. This hypothesis

is coherent, once the wind effect is classified as an exceptional loading for the flare tower design. The results obtained from the analysis confirms the heat radiation levels are below the allowable limits, but the author points that for prolonged exposures these limits must be reviewed. Regarding explosion analysis, Cluttera, Mathisb and Stahl (2007) states that the blast pressure from an open-field explosion event can be estimated with accepted analytical expressions. In this paper Cluttera, Mathisb and Stahl (2007), a numerical formulation is used to model the explosion effects and for the material nonlinearity it was considered an elastoplastic constitutive model for the elements.

According to Fallah and Louca (2007), the pressure-impulse (P-I) diagrams are commonly used in the preliminary design of protective structures to establish safe response limits for given blast-loading scenarios. This P-I diagram is related with a resistance function. The curve obtained from the resistance function presents an elastic-plastic-hardening or softening behavior that can be simplified as bilinear. The area under the curve is related with the P-I. The obtained results have shown that displacement time histories of the proposed analytical models are in good agreement with dynamic results obtained from finite elements analysis.

In the paper of Jia (2011) a structure similar to the flare tower was analyzed under dynamic wind effects (without blast explosion loading). The analyzed structure, called flare boom, is a type of inclined space truss built with tubular elements of stainless steel. The author proves that the wind effects acting on this type of structure can induces the fatigue of structural materials, considering both geometrical, material and load nonlinearities.

Repetto and Solari (2001) developed a probabilistic approach to evaluate the fatigue life of slender vertical structures, such as the flare tower. The authors have pointed to the importance of oscillatory behavior of the stress fields among the structural elements, when subjected to transient loads, and its relation with fatigue. This paper supplies relevant information for the comprehension of the physical phenomenon and the applications to the structural engineering.

The space truss, such as the flare tower, is a structure typically used in situations involving large displacements. When the displacements generated by an action reach a certain level, the structure geometry has a nonlinear behavior in which its stiffness changes due to new internal efforts. Thus, the structure will have two different configurations, the initial and the deformed, which must be taken into account when a project is designed. In these cases, it is not possible to make a superposition of the effects involved due to the difference between these different configurations. It is necessary then to rewrite the equilibrium equations in terms of the deformed configuration. A commonly used solution is done by the linearization of the equilibrium equations, applying algorithms with iterative corrections that use an appropriated convergence criterion.

In the present paper, dynamic actions arising from the impact of shock waves on the flare tower structure during the burning process that occurs inside it is simulated. To formulate the nonlinear kinematics involved in a space truss, the methodology presented in Greco et al. (2012) was used. In this methodology, the Lagrangian description, which considers a fixed reference in space to analyze the structure positions during a certain period of time, is adopted. Firstly, the numerical formulation will be developed for static analysis and in the sequence for the dynamic analysis.

The objective of the paper is to identify the failure mechanism of a flare tower topology and establish its safe conditions.

MATERIAL AND METHODS

The numerical formulation is developed here applying the principle of minimum potential energy. For the static analysis, the total potential energy Π is written in terms of the total strain energy Ut, and in terms of the potential energy of the applied forces, expressed as a function of the applied external forces F and the set of nodal positions X, as shown in Equation (1). Non-conservative forces that realize work could be considered in this functional.

$$\Pi = U_t - FX \tag{1}$$

According to the material elastoplastic constitutive model, the total strain energy U_t is written in Equation (2) for the reference volume V in a fixed referential.

$$U_t = \int_V u dV = \int_V \int_\varepsilon \sigma d\varepsilon dV = \int_V \left(\int_\varepsilon E\varepsilon d\varepsilon - \int_\varepsilon E\varepsilon_P d\varepsilon \right) dV = \int_V \left(\frac{1}{2} E\varepsilon^2 - E\varepsilon\varepsilon_P \right) dV \tag{2}$$

where u is the specific strain energy, σ is the stress tensor, ε is the engineering strain measure, E is the Young modulus and ε_p represents the plastic effects that occur in the body.

In order to derivate the finite element formulation from Equation (1) it is necessary the geometry mapping of the analyzed structure. For the longitudinal strains, the kinematics presented in Figure 1 is parameterized as a function of the non-dimensional variable ξ, which ranges from 0 (for the initial node) to 1 (refer to the end node). Equations (3) to (5) present this kinematical mapping.

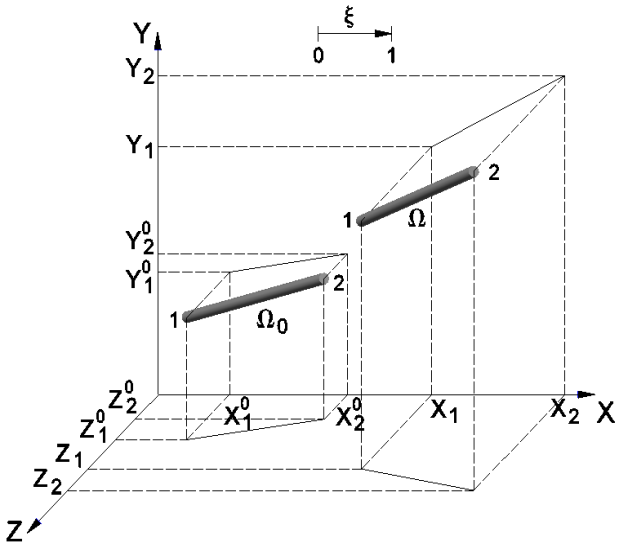

Figure 1: Space truss finite element mapping from its initial position to its deformed position.

$$x = X_1 + (X_2 - X_1)\xi \tag{3}$$

$$y = Y_1 + (Y_2 - Y_1)\xi \tag{4}$$

$$z = Z_1 + (Z_2 - Z_1)\xi \tag{5}$$

For the static nonlinear formulation, the strain measure ε that appears in Equation (2) can be written as a function of the body initial length ds_0, the body deformed length ds and the variable ξ, as shown in Equation (6).

$$\varepsilon = \frac{ds/d\xi - ds_0/d\xi}{ds_0/d\xi} \tag{6}$$

The Equation (2) can be integrated in terms of the cross-sectional area A constant along the finite elements' length, the element's initial length l_0 and the integral along the element's length for specific strain energy over the cross-sectional area, as shown in Equation (7).

$$U = l_0 A \int_0^1 \frac{E}{2} \varepsilon^2 d\xi = l_0 A \int_0^1 u d\xi \tag{7}$$

The total potential energy Π can be rewritten in terms of its nodal positions and conjugated forces, Equation (8), to facilitate the derivative calculations.

$$\Pi = l_0 A \int_0^1 u d\xi - F_{X1}X_1 - F_{Y1}Y_1 - F_{Z1}Z_1 - F_{X2}X_2 - F_{Y2}Y_2 - F_{Z2}Z_2 \tag{8}$$

Then Equation (8) is differentiated in terms of the directions of the degrees of freedom adopted, which can conveniently be equal to the degrees of freedom of the finite elements used in the discretization, and considered it equal to zero. Equation (9) represents the minimum potential energy expression.

$$\frac{\partial \Pi}{\partial X_i} = l_0 A \int_0^1 \frac{\partial u}{\partial X_i} d\xi - F_i = 0 \tag{9}$$

In order to obtain values for the nodal positions of the structure, iterative numerical methods can be used with suitable convergence criterion. Thus, numerical values for the body strains can be calculated.

Non linear positional formulation applied for dynamic analysis

In the case of structures subjected to dynamic loads, the equation that describes the

equilibrium becomes different from that used for the static analysis. Although the formulation developed for U_t in the case of static problems remains valid, other terms appear in the definition of the total potential energy Π. There is one term K_c that refers to the kinetic energy and another term K_a that represents the energy lost due to damping, as shown in Equation (10).

$$\Pi = U_t - FX + \mathrm{K}_c + K_a \tag{10}$$

In the equations that define K_c and K_a an approach is made considering the matrix of discrete mass, according to Oliveira and Greco (2014). Therefore, these equations are represented in Equation (11) and (12).

$$K_c = \int_V \frac{\rho}{2} \dot{X}^2 dV \tag{11}$$

$$\begin{aligned} \mathrm{K}_a &= \int_V c_m \rho X \dot{X} dV - \int_V \int_{X_k} c_m \rho \frac{X\ddot{X}}{\dot{X}} dX_k dV \\ &= CX\dot{X} - C\int_{X_k} \frac{X\ddot{X}}{\dot{X}} dX_k \end{aligned} \tag{12}$$

where ρ is the element's specific mass, M is the global mass matrix, c_m is the damping coefficient, X_k represents the nodal parameters and C is the damping matrix.

To find the equilibrium positions, the minimization of the potential energy is done, now considering the terms which refer to the kinetic energy and to the energy lost due to damping. It was showed in Oliveira and Greco (2014) that the development of this minimization leads to Equation (13).

$$\frac{\partial \Pi}{\partial X} = \frac{\partial U_t}{\partial X} - F + M\ddot{X} + C\dot{X} = 0 \tag{13}$$

In the used formulation, the first term on the right side of Equation (13) is analogous to the resistance function presented in Fallah and Louca (2007). To integrate Equation (13) in time, the Newmark algorithm is used before derivate the equation for the second time considering nodal parameters. For this, the equation is written for a current instant of time S+1, as shown in Equation (14).

$$\left.\frac{\partial \Pi}{\partial X}\right|_{S+1} = \left.\frac{\partial U_t}{\partial X}\right|_{S+1} - F_{S+1} + M\ddot{X}_{S+1} + C\dot{X}_{S+1} \tag{14}$$

The Newmark time integration equations are described in Equations (15) to (17).

$$X_{S+1} = X_S + \Delta t \dot{X}_S + \Delta t^2 \left[\left(\frac{1}{2} - \beta \right) \ddot{X}_S + \beta \ddot{X}_{S+1} \right] \tag{15}$$

$$\dot{X}_{S+1} = \dot{X}_S + \Delta t (1-\gamma) \ddot{X}_S + \gamma \Delta t \ddot{X}_{S+1} \tag{16}$$

$$\ddot{X}_{S+1} = \frac{X_{S+1}}{\beta \Delta t^2} - \frac{X_S}{\beta \Delta t^2} - \frac{\dot{X}_S}{\beta \Delta t} - \left(\frac{1}{2\beta} - 1 \right) \ddot{X}_S \tag{17}$$

where β and γ are constants used to make an approximation in the Newmark time integration equations. In this work, it was adopted a constant average for accelerations in the time steps, i.e. $\gamma = 1/2$ and $\beta = 1/4$.

Replacing Equations (16) and (17) into Equation (14) one has the Equation (18).

$$\left.\frac{\partial \Pi}{\partial X}\right|_{S+1} = \left.\frac{\partial U_t}{\partial X}\right|_{S+1} - F_{S+1} + \frac{M}{\beta \Delta t^2} X_{S+1} - MQ_S + CR_S + \frac{\gamma C}{\beta \Delta t} X_{S+1} - \gamma \Delta t C Q_S \tag{18}$$

where the terms related to the past are represented by Equations (19) and (20).

$$Q_s = \frac{X_s}{\beta \Delta t^2} + \frac{\dot{X}_S}{\beta \Delta t} + \left(\frac{1}{2\beta} - 1 \right) \ddot{X}_s \tag{19}$$

$$R_S = \dot{X}_S + \Delta t (1-\gamma) \ddot{X}_S \tag{20}$$

The second derivative related of Equation (18) in terms of the current positions gives the Hessian matrix, given by Equation (21), as presented in Greco et al. (2012).

$$\left.\frac{\partial^2 \Pi}{\partial X^2}\right|_{S+1} = \nabla g\left(X^0\right) = \left.\frac{\partial^2 U_t}{\partial X^2}\right|_{S+1} + \frac{M}{\beta \Delta t^2} + \frac{\gamma C}{\beta \Delta t} \tag{21}$$

Equation (18) is nonlinear regarding spatial variables (X). To solve Equation (18) the Newton-Raphson iterative method can be applied, as described in Equations (22) and (23). Thus, the values of equilibrium positions of the structure subjected to dynamic load are calculated. From this, ΔX values are obtained, which are used to correct the new values of the nodal positions and accelerations in the current step S+1, as described in Equations (24) and (25). Then, these values are taken to Equations (15) and (16), so that the positions in the next step can be calculated.

$$g(X) \cong 0 \cong g(X^0) + \nabla g(X^0)\Delta X \tag{22}$$

$$g(X^0) = \left.\frac{\partial U_t}{\partial X}\right|_{S+1} - F_{S+1} + \frac{M}{\beta\Delta t^2}X_{S+1} - MQ_S + CR_S + \frac{\gamma C}{\beta\Delta t}X_{S+1} - \gamma\Delta t C Q_S \tag{23}$$

$$X_{S+1} = X_S + \Delta X \tag{24}$$

$$\ddot{X}_{S+1} = \frac{X_{S+1}}{\beta\Delta t^2} - Q_S \tag{25}$$

For ΔX values of the iterative method be evaluated as sufficiently small and then move up to the next step, the stopping criterion must be defined as shown in Equation (26). When this criterion is reached, the calculated values for S+1 become the past values S.

$$\sqrt{\sum_{i=1}^{coord} g^2(X^0)} \le TOL \tag{26}$$

Before initiate the first step, initial nodal accelerations must be calculated according to Equation (27).

$$\ddot{X}_0 = M^{-1}\left[F_0 - C\dot{X}_0 - \left.\frac{\partial U_t}{\partial X}\right|_0\right] \tag{27}$$

Equivalent actions due to explosions

The process of the combustion of gases that occurs inside the flare tower violently releases a volume of compressed gas. The energy involved in this process is spread in the air, generating pressure variations and explosive waves, known as shock waves, which reach the tower surface. The behavior of the pressure that a shock wave exerts on the surface is shown in Figure 2. The wave is formed at the time of the explosion and it moves up to the surface at time t_A, when it passes immediately to exerts a high pressure on the object (overpressure peak P_{so}), which decays exponentially to a negative pressure phase known as suction region. After this suction region, there is the stabilization whit return to the ambient pressure.

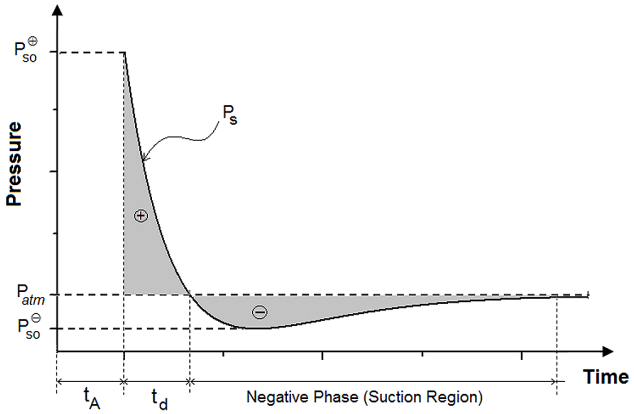

Figure 2: Transient pressure behavior for an explosive wave from the point of view of an observer or target.

The Shock Wave method presented in TNO PrinzMauritz Institute (1997) models the behavior of explosions that specifically involve gases. In this method, the values of the shock wave overpressure peak P_{so} is defined in Equation (28).

$$\frac{P_{s0}}{P_{atm}} = \phi\frac{L_0}{x} \tag{28}$$

where P_{atm} is the atmospheric pressure, ϕ is the reactivity level of the gas in accordance with Table 1, L_0 is the characteristic length given by Equation (29) and x is the distance from the point taken to the center of explosion.

$$L_0 = \left[\frac{V_0 E_{VC}}{P_{atm}}\right]^{\frac{1}{3}} \tag{29}$$

where V_0 corresponds to the volume occupied by the gas-air stoichiometric mixture calculated by Equation (30) and E_{VC} is the specific energy of the combustion.

$$V_0 = \frac{(1+5n)\cdot m \cdot R \cdot T}{Mm \cdot P_{atm}} \quad (30)$$

where m is the mass of gas, R is the universal gas constant, T is the temperature of the mixture, Mm is the molecular weight of the gas and n is the number of moles required for stoichiometric reaction O_2.

Table 1: Values of the reactivity ϕ of gases and the rate of flame spread uf, according to TNO PrinzMauritzInstitute (1997).

Reactivity	*uf*(m/s)	ϕ	Example of gases
Low (A)	40	0.02	Methane, Carbon monoxide, etc.
Medium (B)	80	0.06	Ethane, propane, butane, etc.
High (C)	160	0.15	Hydrogen, acetylene, ethene oxide, etc.

The duration of the positive phase t_d is defined by Equation (31).

$$t_d = \frac{L_0}{a}\left[0.456\left(\frac{a}{u_f}-1\right)+\frac{3\phi}{7}\ln\left(\frac{1+\frac{7}{3\phi}\cdot\frac{x}{L_0}}{1+\frac{1.064}{\phi}}\right)\right] \quad (31)$$

where a is the speed of sound in the air.

The function that describes the decay of the force is defined in Equation (32).

$$F(t) = \frac{P_{S0}}{S}\left(1-\frac{t}{t_d}\right)e^{\frac{-t}{t_d}} \quad (32)$$

where S is the area in which the pressure from the shock waves acts.

New and more accurate methods to evaluate accidental loads on offshore structures can be found in Hirdaris (2015) and Czujko and Paik (2015).

The analyzed flare tower structure

For the simulation of the efforts in the flare tower, the dimensions of a new structure were calculated according to the norm American Petroleum Institute API 521(2007), which establishes the tower diameter, pilot flame length, flame distortion caused by the action of winds and minimum tower height. From data obtained from Gilmer et al. (2003), it was obtained a diameter of 1.31 m and height of 65.8 m.

For the positioning of the nodes and elements that make up the flare tower, geometry similar to the tower of the Petrobras platform P-55, currently under construction to serve in Campos' Basin - RJ, was used because its comparable size to those obtained in the calculations (height: 65.8 m divided in 12 equally spaced modules; area of the base: 7.80 m; area of the top: 6.52 m). The structure was considered to be composed by 39 nodes and 108 elements arranged as shown in Figure 3. The considered elements are tubes with a diameter of 168 mm, thickness of 7.1 mm, cross-sectional area of 3.6 x 10^{-3} m², moment of inertia of 1.71 x 10^{-5} m⁴ and stainless steel composition with properties as shown in Table 2.

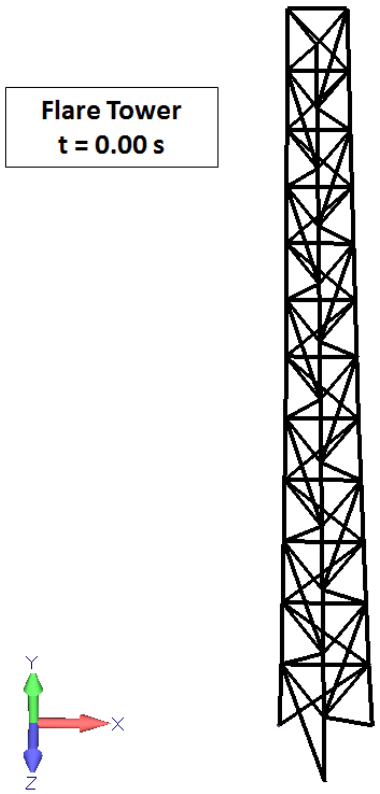

Figure 3: Flare tower used in the simulation.

Table 2: Physical properties of Stainless Steel, according to Gerdau (2015).

σ_{yield}(MPa)	$\sigma_{resistance}$(MPa)	*E*(GPa)	ρ(kg/m³)
355	500	200	7850

The damping values and Euler critical load for each element were also calculated. It was considered that the damping ratio equal to 1%, reasonable for applications in metal structures.

The numerical simulations were performed using an original code programmed by the authors of the paper. The initial source code presented in Greco, Ferreira and Barros (2013) was developed in Fortran language for dynamic analysis of space structures with nonlinear behavior. This code was modified to include blast loads generated by the combustion of gases at the top of flame tower.

The damping rate (ξ) presented in Equation (33) is associated to the damping coefficient (c_m) through the finite element fundamental frequency (ω).

$$\xi = \frac{c_m}{2\omega} \tag{33}$$

For the truss finite element, the fundamental frequency can be evaluated by Equation (34).

$$\omega = \frac{1}{L_0}\sqrt{\frac{E}{\rho}} \tag{34}$$

The Euler critical load as defined by Equation (35).

$$P_{CR} = \frac{\pi^2 EI}{l_o} \tag{35}$$

where I corresponds to the minimum inertia moment of the element. The tangent stiffness is used to caculate the critical load when plastic strains occur.

RESULTS AND DISCUSSION

To simulate the stress that appear in the tower, it was defined as tolerance in iterative stopping criterion a value equal to 10^{-8} and time steps for integration equal to 0.001s. The action of forces was divided into two phases. In the first phase, lasting 1.05s an initial and decreasing force equal to 1000 kN, distributed among the three nodes located at the top of tower, as shown Figure 4. In the second phase, it was considered a free vibration condition (without prescribed forces) so that it oscillates until return to its equilibrium position.

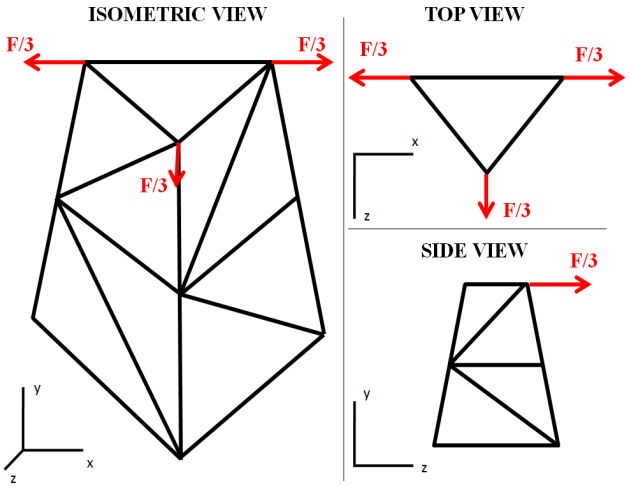

Figure 4: Distribution of the forces located at the top of the tower.

The simulation generated stress and stain results with which curves were plotted as shown in Figures 5 and 6. The responses shown that for an element located close to the medium height of the structure, the one that presented the most representative absolute values.

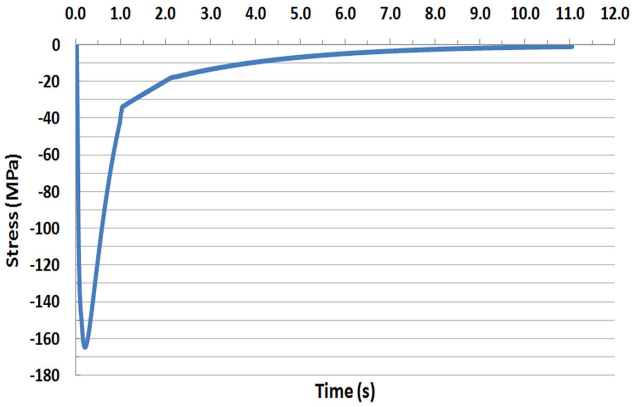

Figure 5: Normal stress transient analysis.

The complete result analysis indicates that none of the elements have reached the yield stress of 355 MPa.Thus, no plastic deformation occurred. The similarity between the stress and strain curves indicated a material linearity characteristic of the elastic behavior. As the tower was subjected to explosions permanently, this result was already expected.

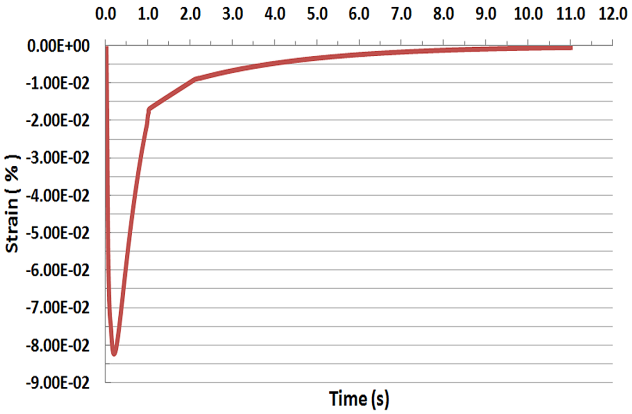

Figure 6: Normal strain transient analysis.

The obtained values also indicated that the compressive forces acting on the elements were below their Euler critical load. Therefore, it was possible to conclude that no buckling occurred in the flare tower structure.

After the simulation, the displacements values of the structure nodes were also obtained. In Figure 7, it is shown the tower in time 0.18 s, when its highest normal strain level occurred. The images of the structure in its initial (black) and deformed state (blue) were overlaid in order to facilitate the visualization of the effects generated. It can be observed that the displacements were quite small.With the displacements values it was possible to plot curves that showed the structure behavior in the x, y and z directions, as well as their respective phase figures. In Figure 8, the displacements of a node situated at the top of the flare tower are presented (in the z direction). This node presents the largest displacements among the structural nodes. In Figure 9, the phase figure for this displacement is shown.

It is noted that when the explosion finishes at time 1.05 s, the tower returns to its initial position without the occurrence of free vibration phase remarkable, probably caused by the damping ratio of 1 % that may have over-damped the structure. After reach the largest displacement of -0.37116 m, it is possible to see in Figure 9 that the structure returns to its initial position (displacement equal to zero) without oscillation. Even if it had had a free vibration phase, this fact would not occur in a real situation due to the action of a new explosion subsequent to the first, which would interrupt the return of the structure to its initial position.

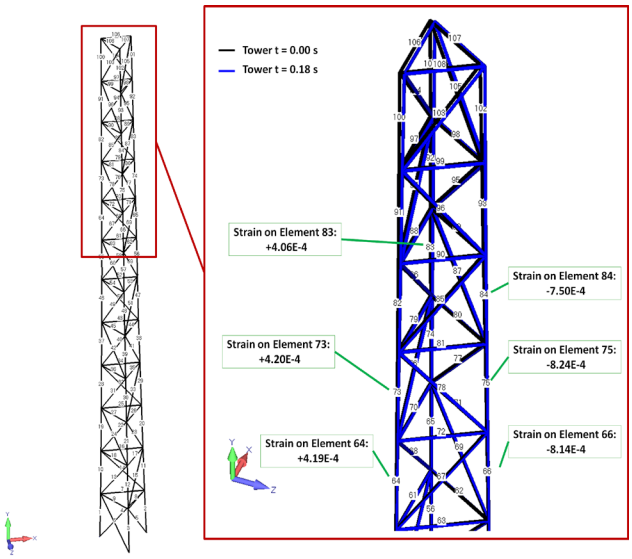

Figure 7: Tower deformed at time 0.18 s and the strain in the most representative elements.

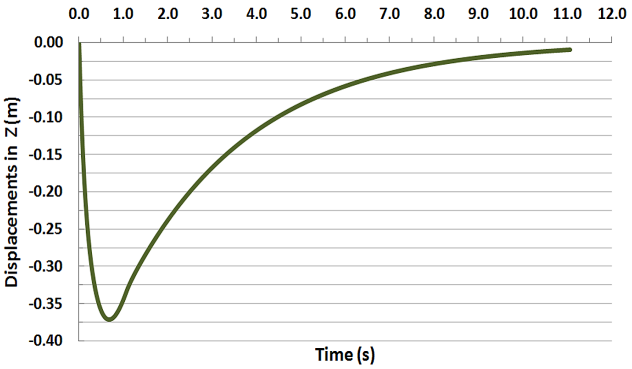

Figure 8: Transient analysis of the displacements in the z direction.

During the process of petroleum extraction, an uncountable number of explosions occur inside the flare tower as indicate the permanent pilot flame lit for most part of the time. The highest stress of 165 MPa verified during the simulation was then considered as the alternating stress that acts on the tower structure, so that an estimate could be made for the number of cycles that would indicate the tower lifetime considering fatigue. According to *Branco, Fernandes* and *Castro* (1999), the σ-n curve for the structural steel indicates that the alternating stress is below the limit of 200 MPa for the durability limit of structural steel. However, considering a lifetime of 10^8 cycles and the duration for each burst of 1.05 s, a lifetime of 3 years would be estimated. After this period, an evaluation of the maintenance in the structure would be necessary.

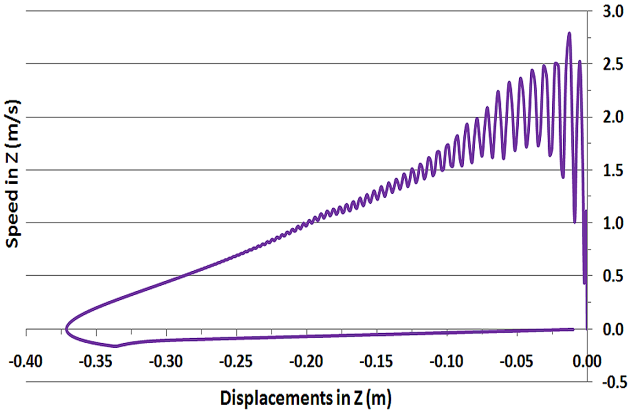

Figure 9: Phase figure for the displacements in z direction for critical top nodal point.

The values found for stresses in the structure indicated that it was projected with a good margin of safety, considering that the maximum stress verified of 84 MPa for traction and 165 MPa for compression correspond for up to 46% of the yield stress of 355 MPa for the material considered. In addition, the maximum alternating stress of 165 MPa corresponded to 83% of the limit of durability for the material fatigue, which has been indicated that the structure resists to the efforts generated on the simulation analyzed in this paper. However, it should be noted that only dynamic loads resulting from the explosions that occur inside the flare tower was considered. In a full structural analysis, exceptional efforts resulting from winds, oscillations due to tidal action in the base of the platforms and others dynamic loads should be also taken into account. Moreover, the stiffness of whole platform or ship structure must be taken into account for the full structural analysis.

Technical standard Eurocode3 (2001) limits the maximum lateral displacement in tower up to 2% of the structure height, as shown in Equation (36).

$$\delta_{MAX} = \frac{h}{50} \tag{36}$$

where h is the tower height.

This lateral displacement is limited to avoid excessive second order effects acting in the structural system. In the case of the analyzed tower, Equation (37) presents the maximum lateral displacement allowed.

$$\delta_{MAX} = \frac{65.8}{50} = 1.316m \tag{37}$$

The maximum lateral displacement obtained in the analysis (almost 0.4 m according to Figure 8) is smaller than the maximum lateral displacement allowed in the Eurocode3 standard. Thus this displacement is covered by the Eurocode3 in terms of accidental limit state.

Regarding the errors of the performed modeling, they can be classified as physical, geometrical and due to initial/boundary conditions. The physical error is related to the properties of materials (characteristic stresses, young modulus and density), besides the homogeneity of materials used in the elements. This kind of error is minor and can be considered reducing the stiffness of the elements. The geometrical error is related to imperfections due to the building process and it is more relevant as larger initial stresses were introduced in the structure. For real applications, these imperfections must be considered in the design through horizontal initial displacement on the top of the tower or through horizontal equivalent forces, as presented inthe technical procedure ABNT NBR 8880 (2008). Regarding initial conditions, several uncertainties are involved in the analysis, such as the gas constitution and the burn conditions. The adopted method is conservative regarding these uncertainties. Regarding the boundary conditions, the adopted truss idealization also presents another source of approximation, but again it is conservative regarding the structural design.

CONCLUSIONS

The flare tower has a good resistance when it is subjected to dynamic actions caused by shock waves originated during explosions that occur inside it. During the simulation, stress values obtained indicated that plastic deformation, buckling and fatigue failure do not occur. In addition, the displacements curve indicated that an accentuated free vibration phase does not occur, probably due to the damping rate of 1% considered, which may have over-damped the structure. Even if a free vibration phase were detected, it would not occur actually due to the action of a subsequent explosion that would not

allow the structure to return to its initial position. The nonlinear positional formulation used in this paper was valid for simulation of dynamics efforts since it have been presented consistent results.

High temperature sources are important factors in thermomechanical analysis regarding the structures with elastoplastic behavior. It stands out the accumulation of irreversible strains because, depending on the history of the strain fields, a portion of a significant amount of heat is generated. It is emphasized the consideration of thermomechanical unidirectional coupling associated to the blast problems in which, due to high strain rates, promotes significant effects in the interaction between the mechanical and thermal response, modifying the structural behavior. Therefore, for future works, it is clear the importance of thermomechanical coupling in problems engineering, because, depending on the material, loading and initial conditions, such coupling may provide structural predominant contributions to the response. A major difficulty to model this coupling is the complex behavior of the flame and the heat propagation in the structural environment. According to Westbrook et al. (2005), the complexity of combustion models are related to different combinations of greater spatial resolution, more chemical species, a more complex turbulence model, a more sophisticated radiation model, multiple phase phenomena or moving objects.

In the current paper, truss elements were considered to model the structure. For these jointed elements, the structural analysis is more conservative and differences mainly related to natural frequencies and structural vibrations are noted. To improve the structural system modeling, the Timoshenko beam elements can be used instead of the truss elements. But with higher computational cost and, for these beam elements, some mechanical approximation still prevails (i.e. the shear stress along cross-sectional height are evaluated through a mean value). According to Hirdaris and Lees (2005), to improve the shear stress distribution, a consistent higher-order beam theory could be used. Moreover, Hirdaris and Lees (2005) presents a high order plane finite element suitable for the calculation of natural frequencies of complex free vibrating continuous systems.

ACKNOWLEDGEMENTS

The authors would like to acknowledge CNPq (National Council of Scientific and Technological Development) and FAPEMIG (Minas Gerais State Research Foundation) for financial supports, under grant numbers 302376/2016-0, 441573/2014-2 and TEC-PPM-00409-16.

REFERENCES

AMERICAN PETROLEUM INSTITUTE API 521. **Guide for pressure-relieving and depressuring systems**. API Recommended Practice. 5th ed., 2007.

ASSOCIAÇÃO BRASILEIRA DE NORMAS TÉCNICAS – ABNT NBR 8880. **Projeto de estruturas de aço e de estruturas mistas de aço e concreto de edifícios**. 2008.

BRANCO, C. M.; FERNANDES, A. A.; CASTRO, P. **Fadiga de estruturas soldadas**. 2nd ed. Lisboa: Fundação de Calouste Gulbenkian, 1999.

CLUTTERA, J. K.; MATHISB, J. T.; STAHL, M. W. Modeling environmental effects in the simulation of explosion events. **International journal of impact engineering**, 34(5): 973–989, 2007.

CZUJKO J.; PAIK, J. K. A new method for accidental limit states design of thin-walled structures subjected to hydrocarbon explosion loads. **Ships and Offshore Structures**, Special issue on Loads for Ships and Offshore Structures, 10(5): 460-469, 2015.

EUROCODE3. **Design of steel structures – S.l**. 2001.

FALLAH, A. S.; LOUCA, L. A. Pressure–impulse diagrams for elastic-plastic-hardening and softening single-degree-of-freedom models subjected to blast loading. **International journal of impact engineering**, 34(4): 823–842, 2007.

GERDAU. **Perfis estruturais Gerdau –** Informações técnicas. Brasil, 2015.

GILMER, L. K.; CAICO, C. A.; SHERRICK, J. J.; MUELLER, G. R.; LOOS, K. R. **Draft flare waste gas flow and composition measurement methodologies evaluation document**. Texas Commission on Environmental Quality, Work assignment 5. Prepared by Shell Global Solutions, Houston,

Texas, 2003. Available in: https://pt.scribd.com/document/266069169/Flare-Waste-Gas-Flow-Rate. Access in: May, 12, 2017.

GRECO, M.; FERREIRA, I. P.; BARROS, F. B. A classical time integration method applied for solution of nonlinear equations of a double-layer tensegrity. **Journal of the Brazilian Society of Mechanical Sciences and Engineering**, 35(1): 41-50, 2013.

GRECO, M. et al. Comparison between two geometrical nonlinear methods for truss analyses. **Structural Engineering andMechanics**, 41(6): 735-750, 2012.

HIRDARIS, S. E. Loads on ships and offshore structures. **Ships and Offshore Structures**, 10(5): 459 (Editorial), 2015.

HIRDARIS, S. E.; LEES, A. W. A unified conforming finite element forthe vibration of thick beams and frames. **International Journal for Numerical Methods in Engineering**, 62(4): 579-599, 2005.

JIA, J. Wind and structural modelling for an accurate fatigue life assessment of tubular structures. **Engineering structures**, 33(2): 477–491, 2011.

KINNEY, G. F.; GRAHAM, K. J. **Explosive Shocks in Air**. New York: Springer-Verlag, 1985.

OLIVEIRA, F. M.; GRECO, M. Nonlinear dynamic analysis of beams with layered cross sections under moving masses. **Journal of the Brazilian Society of Mechanical Sciences and Engineering**, 37(2): 451-462, 2014.

REPETTO, M. P.; SOLARI, G. Dynamic along wind fatigue of slender vertical structures. **Engineering structures**, 23(12):1622–1633, 2001.

SINGHAL, S. N. Offshore stack-enclosed gas flares: part II - application and results. **Fire safety journal**, 15(3): 227-244, 1989.

TNO PRINZ MAURITZ INSTITUTE. **Methods for the Calculation of the Physical Effects of the escape of dangerous materials (liquid and gases) – Part II**. Yellow Book, 3rd ed., 1997.

WESTBROOK, C. K. et al. Computational combustion. **Proceedings of the Combustion Institute**, 30(1): 125–157, 2005.